variable threshold function in order to eliminate the deadband. The others are used for attenuation using the weighted sum operation of the FG-MOSFETs. When $w_{in} = w_{ip} = w_i$, from eqn. 2, V_f of FM_n (V_{fn}) and FM_p (V_{fp}) are given by

$$V_{fn} = V_{in}(D_0 w_1 + D_1 w_2 + D_2 w_3) + w_4 V_{Bn} \qquad (4)$$

$$V_{fp} = V_{in}(D_0 w_1 + D_1 w_2 + D_2 w_3) + w_4 V_{Bp} \qquad (5)$$

where D_0, D_1 and D_2 are the digital signals and are equal to 1 or 0. If $V_{Bn} \geq V_{Tn}/w_4$ and $|V_{Bp}| \geq |V_{Tp}|/w_4$ are satisfied, the polarities of V^*_{Tn} and V^*_{Tp} are changed, and so both FM_n and FM_p operate as depletion-mode MOSFETs. Consequently, the current operates as a Class AB circuit so that each conducts a small quiescent current for $V_{in} = 0$. Therefore, the deadband can be eliminated perfectly. When we design $w_1{:}w_2{:}w_3 = 2^0{:}2^1{:}2^2$, from eqns. 4 and 5, the ideal V_{out} can be given by

$$V_{out} = V_{in} w_1 \sum_{j=0}^{2} D_j 2^j + I_{RL0} R_L \qquad (6)$$

where I_{RL0} is I_{RL} at $V_{in} = 0$. From eqn. 6, the circuit operates as a digitally programmable Class AB attenuator.

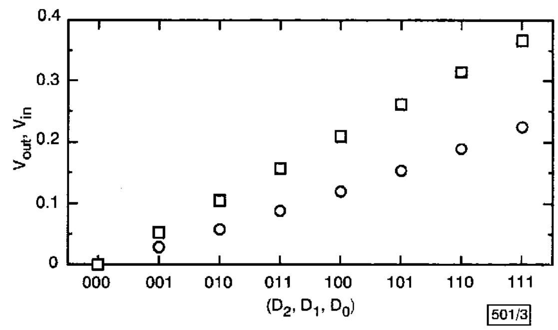

Fig. 3 *Gain against (D_2, D_1, D_0)*

□ without R_L
○ R_L = 10kΩ

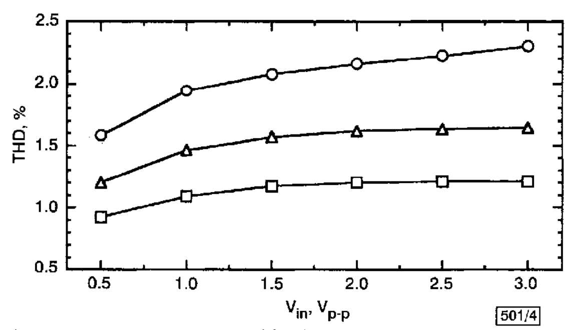

Fig. 4 *THD against input signal level*

—□— (D_2, D_1, D_0) = (0, 0, 1)
—△— (D_2, D_1, D_0) = (1, 0, 0)
—○— (D_2, D_1, D_0) = (1, 1, 1)

Simulation and experimental results: The proposed circuit was evaluated using HSPICE simulation with 0.6μm CMOS process parameters (LEVEL 28). In this simulation, W/L of FM_n and FM_p were 40μm/3μm and 80μm/3μm, respectively. To satisfy $w_{in} = w_{ip}$, we used a sufficiently large C_4 to satisfy $C_4 \gg C_0$, and the value of which was 3pF. The other weighted capacitors and supply voltage were $C_3 = 2C_2 = 4C_1$ = 250fF and $V_{DD} = -V_{SS} = V_{Bn} = -V_{Bp}$ = 1.5V, respectively. Fig. 3 shows the relationship between the gain of the circuit and (D_2, D_1, D_0). It has high linearity and has variable gain range of –13dB to –31dB when R_L = 10kΩ. The total harmonic distortion (THD) against input signal level at R_L = 10kΩ is shown in Fig. 4. In the simulation, a 3V_{p-p}, 500kHz input signal at (D_2, D_1, D_0) = (1,1,1) resulted in a THD below 2.3%. The –3dB bandwidth with R_L = 10kΩ and the total static power consumption without loads were 11.5MHz and 14.3μW, respectively. The proposed attenuator was also verified experimentally using discrete devices. In the experiment, $V_{DD} = -V_{SS} = V_{Bn} = -V_{Bp}$ = 3V, R_L = 10kW, $C_3 = 2C_2 = 4C_1$ = 0.1μF and C_4 = 0.44μF were used. Fig. 5 shows an oscilloscope photograph of the circuit with a 6V_{p-p} triangular wave input. This photograph shows that the experimental circuit operates well as an attenuator without a deadband. The variable gain range of the circuit was –5.0dB to –20.5dB.

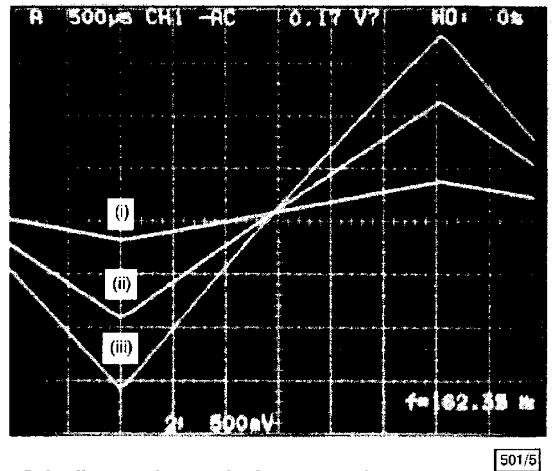

Fig. 5 *Oscilloscope photograph of experimental circuit*

(i) (D_2, D_1, D_0) = (0, 0, 1)
(ii) (D_2, D_1, D_0) = (1, 0, 0)
(iii) (D_2, D_1, D_0) = (1, 1, 1)

Conclusion: A simple digitally programmable attenuator using FG-MOSFETs has been proposed. The device is very useful for analogue signal processing systems.

12 March 2001
Electronics Letters Online No: 20010416
DOI: 10.1049/el:20010416

K. Tanno, H. Tanaka, M. Syuto and O. Ishizuka (*Faculty of Engineering, Miyazaki University, 1-1 Gakuenkibanadai-nishi, Miyazaki-shi 889-2192, Japan*)

E-mail: tanno@esl.miyazaki-u.ac.jp

References

1 QIN, S., and GEIGER, R.: 'A ±5-V CMOS analog multiplier', *IEEE J. Solid-State Circuits*, 1987, **SC-22**, (6), pp. 1143–1146
2 OTAKA, S., TANIMOTO, H., WATANABE, S., and MAEDA, T.: 'A 1.9-GHz Si-bipolar variable attenuator for PHS transmitter', *IEEE J. Solid-State Circuits*, 1997, **32**, (9), pp. 1424–1429
3 GRAY, P.R., and MEYER, R.G.: 'Analysis and design of analog integrated circuits' (John Wiley & Sons, 1993), 3rd edn., Chap. 5
4 SHIBATA, T., and OHMI, T.: 'A functional MOS transistor featuring gate-level weighted sum and threshold operation', *IEEE Trans. Electron Devices*, 1992, **39**, (6), pp. 1444–1455

ZVT-PWM boost converter for unity power factor applications

C.C. Wu and C.M. Young

A new single-phase ZVT-PWM boost converter with an active snubber is proposed to achieve unity power factor operations for a wide load range. The unique location of the resonant inductor and capacitor ensures that low switching stress and commutation losses are obtained in the converter. The proposed converter is suitable for high power factor correctors.

Introduction: In recent years, various soft-switching techniques have been proposed to reduce switching losses and EMI noise in switching mode converters. The zero voltage transition-pulsewidth modulation (ZVT-PWM) converters introduced in [1, 2] have been the most successful. They combine desirable features of both the conventional PWM and the soft switching resonant technique.

Soft switching commutation is achieved in the main switch and, as a result, the power losses and EMI are reduced considerably. However, the auxiliary switch in [1] is turned off with hard switching. In [2], the voltage across the auxiliary switch is higher than the output voltage. To overcome these disadvantages, a new single-phase ZVT-PWM boost converter is suggested in this Letter. This converter is able to improve on the disadvantages of the conventional ZVT-PWM boost converter [1, 2].

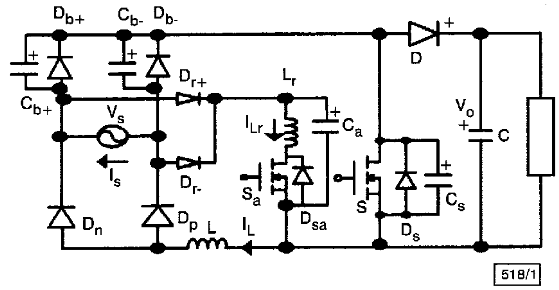

Fig. 1 *Circuit diagram of proposed converter*

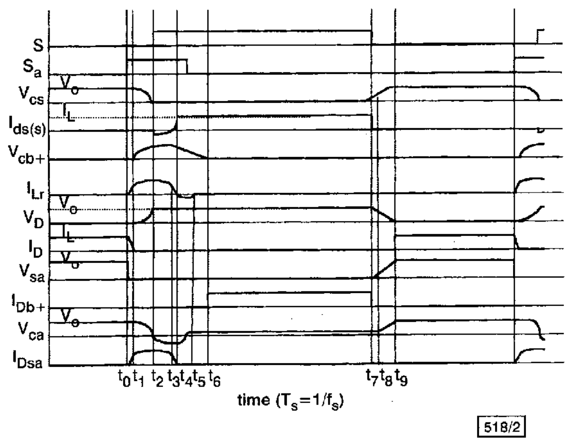

Fig. 2 *Theoretical waveforms of proposed converter*

Proposed converter: The main circuit topology is depicted in Fig. 1. The proposed converter is the combination of the conventional PWM boost converter and the active snubber resonant branch. When the input line is positive (or negative), D_{b-} (or D_{b+}), D_{r-} (or D_{r+}) and D_n (or D_p) are always turned off, D_{b+} (or D_{b-}), D_p (or D_n), D_{r+} (or D_{r-}), D and S perform the boost function with power factor correction. This converter differs from the conventional one. The changed location of the resonant inductor, capacitor and diode ensure low current and voltage stresses in the converter. In order to simplify the analysis, it is assumed that all the components are ideal ($C_{b+} = C_{b-} = C_b > C_s$) and L is treated as a constant current source I_L. For convenience in analysing the proposed converter, we will consider only the positive half-cycle of the input source. The circuit operation in one switching cycle can be divided into ten stages, and the key operating waveforms of the proposed converter are shown in Fig. 2.

Stage (i) (t_0, t_1): Prior to t_0, S and S_a are off, D is conducting. At t_0, S_a is turned on in a zero current switching (ZCS) way and $I_{Lr}(t)$ rises linearly from zero to I_L. At t_1, D and D_{b+} are turned off with soft commutation.

Stage (ii) (t_1, t_2): This is the resonant stage. The first resonant path is C_s–C_{b+}–D_{r+}–L_r–S_a–C_s, and the second resonant path is C_a–L_r–S_a–C_a. During this stage, C_s and C_a are discharged, and C_{b+} is charged, then the growth rate of the voltage across D is restricted by the voltage across C_s to achieve zero voltage switching (ZVS) turn off. At t_2, the voltage on S is zero, which is the end of this stage.

Stage (iii) (t_2, t_3): This stage begins when S is turned on at ZVS form. The resonance between L_r, C_a, and C_{b+} continues through D_{r+}, S_a, and D_s. This stage finishes when $I_{Lr}(t)$ reaches I_L again.

Stage (iv) (t_3, t_4): In this stage, the current in S_a falls from I_L to zero while the current in S rises from zero to I_L. This stage ends when $I_{Lr}(t)$ is equal to zero.

Stage (v) (t_4, t_5): During this stage, C_{b+} is linearly discharged by I_L and the resonance between L_r and C_a continues through D_{Sa}, S_a can be turned off in a ZVS way. This stage finishes when $I_{Lr}(t_5) = 0$.

Stage (vi) (t_5, t_6): During this stage, C_{b+} continues to linearly discharge by I_L through S. It finishes when the voltage on C_{b+} is zero.

Stage (vii) (t_6, t_7): This stage begins when D_{b+} is turned on in a ZVS way. The circuit operation is identical to the turn-on behaviour of a conventional PWM boost converter.

Stage (viii) (t_7, t_8): This stage begins when S is turned off and ends when $V_{Cs}(t)$ is charged to $V_{ca}(t_5)$. During this stage, C_s is charged linearly and the growth rate of the voltage across S is limited.

Stage (ix) (t_8, t_9): During this stage, C_s and C_a are charged linearly by current I_L. It finishes when $V_{Cs}(t)$ and $V_{ca}(t)$ is charged to V_o.

Stage (x) (t_9, t_0): This stage begins when D is turned on under ZVS. The operation of the circuit at this stage is identical to the normal turn-off operation of a PWM boost circuit. It ends at the moment that S_a is turned on to begin a new switching cycle.

Based on the circuit analysis presented above, the proposed active snubber is activated only during the short ZVT transient; the ZVT-PWM converter is identical to a common PWM converter most of the time. Moreover, this converter can be easily built in conjunction with a power factor correction circuit.

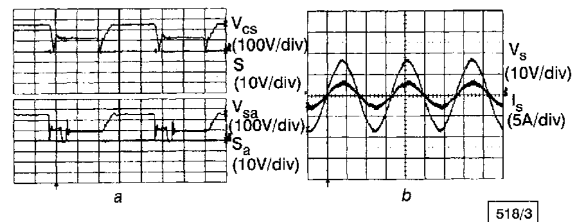

Fig. 3 *Measured waveforms of proposed converter*

a Experimental results of proposed converter
Time: 1µs/div
b Waveform of input line voltage and line current
Time: 5ms/div

Experimental results: A 250W prototype of the proposed converter was built and tested (V_s = 120V_{rms}, V_o = 250V, L_r = 6µH, C_{b+} = C_{b-} = 22nF, C_s = 2nF, C_a = 2nF, L = 740µH, C = 680µF, f_s = 100KHz). The key experimental results of the proposed converter are shown in Fig. 3*a*. It can be seen that the experimental waveforms are relatively clean and agree with the theoretical analysis waveforms very well. The main switch is turned on and turned off with ZVS. The auxiliary switch is turned on with ZCS and turned off with ZVS. The conversion efficiency was found to be 92% at the rated load. Fig. 3*b* shows the waveform of the input line voltage and line current. The input power factor is nearly unity.

Conclusions: A new ZVT-PWM boost converter using an active snubber has been proposed and tested. Its salient features are as follows: (i) soft switching operation can be easily maintained for a wide line and load range; (ii) there are low switching stress and commutation losses in the converter, and (iii) the auxiliary snubber circuit is simple.

 12 March 2001

Electronics Letters Online No: 20010427
DOI: 10.1049/el:20010427

C.C. Wu and C.M. Young (*Department of Electrical Engineering, National Taiwan University of Science and Technology, 43, Keelung Road, Sec. 4, Taipei, Taiwan 106, Republic of China*)

E-mail: young@mouse.ee.ntust.edu.tw

References

1 HUA, G., LIEU, C.S., JIANG, Y., and LEE, F.C.: 'Novel zero-voltage-transition PWM converter', *IEEE Trans. Power Electron.*, 1994, **9**, (2), pp. 213–219

2 YANG, L., and LEE, C.Q.: 'Analysis and design of boost zero voltage transition PWM converter'. IEEE Power Electron. Spec. Conf Rec., 1993, pp. 707–713